Supporting information

Controlled synthesis of telechelic polypeptides *via* polymerization of *N*-carboxyanhydrides mediated by phosphate kinetic modulators

Tingting Cao[a,b,c,d], *Chenlin Ji*[b,c,d], *Qianyi Qin*[b,c,d], *Hui Wang*[b,c,d], *Yu Zhao*[b,c,d*], *Ziyuan Song*[e*], *Jianjun Cheng*[b,c,d*]

[a] School of Materials Science and Engineering, Zhejiang University, Hangzhou, China

[b] Research Center for Industries of the Future and [c] Department of Materials Science and Engineering, Westlake University, Hangzhou, China

[d] Institute of Advanced Technology, Westlake Institute for Advanced Study, Hangzhou, China

[e] Institute of Functional Nano & Soft Materials (FUNSOM), Jiangsu Key Laboratory for Carbon-Based Functional Materials and Devices, Soochow University, Suzhou, China

*Corresponding authors: chengjianjun@westlake.edu.cn; zysong@suda.edu.cn; zhaoyu51@westlake.edu.cn

Materials

Amino acids, formic acid, acetic acid and caprylic acid were purchased from Tokyo Chemical Industry (Shanghai, China). Triphosgene, propylene oxide, diphenyl phosphate (DPP), dimethyl phosphate (DMP), and diphenyl carbonate (DPC) were purchased from Shanghai Macklin Biochemical Technology Co., Ltd. (Shanghai, China). 1,3-Diaminopropane (C_3-diNH_2), 1,6-diaminohexane (C_6-diNH_2), 1,12-dodecanediamine (C_{12}-diNH_2) and PEG-diamine (PEG_{1000}-diNH_2) were purchased from Millipore Sigma Chemical Co. (St. Louis, MO, USA). Deuterated solvents were purchased from Cambridge Isotope Laboratories, Inc. (Tewksbury, MA, USA). Other commercial reagents were purchased from Shanghai Aladdin Biochemical Technology Co., Ltd. (Shanghai, China). All reagents were used as received unless otherwise specified. Monomers including γ-benzyl-$_L$-glutamate *N*-carboxyanhydride (BLG-NCA), γ-ethyl-$_L$-glutamate *N*-carboxyanhydride (ELG-NCA), N^{ε}-benzyloxycarbonyl-$_L$-lysine NCA (ZLL-NCA), and γ-benzyl-$_D$-glutamate *N*-carboxyanhydride (BDG-NCA) were synthesized following literature procedures [1, 2].

Instruments

^{1}H nuclear magnetic resonance (^{1}H NMR) and ^{31}P nuclear magnetic resonance (^{31}P NMR) spectra were recorded on a 600 MHz-Solution NMR Spectrometer in Westlake University. Chemical shifts (δ) were reported in ppm and referenced to the residual protons in deuterated solvents. MestReNova software (version 14.0.0, Mestrelab Research, Escondido, CA, USA) was used for all NMR analysis. Gel permeation chromatography (GPC) experiments were performed on a system equipped with an isocratic pump (1260 Infinity II, Agilent, Santa Clara, CA, USA), a multi-angle laser light scattering (MALLS) detector (DAWN HELEOS-II, Wyatt Technology, Santa Barbara, CA, USA), and a differential refractive index (dRI) detector (Optilab, Wyatt Technology, Santa Barbara, CA, USA). The detection wavelength of HELEOS was set at 658 nm. Separations were performed using serially connected size exclusion columns (three Shodex packed columns KD-803, KD-804 and KD-805, 10 μm, 8 × 300 mm, Yokohama, Japan) using DMF containing LiBr (0.1 M) as the mobile phase at a flow rate of 1.0 mL/min at 50 °C. The MALLS detector was calibrated using pure toluene

and can be used for the determination of the absolute molecular weights (MWs). The MWs of polymers were determined based on the d*n*/d*c* value of each polymer sample using the internal calibration system processed by the ASTRA software (Version 8.12, Wyatt Technology, Santa Barbara, CA, USA). Fourier transform infrared (FT-IR) spectra were recorded on a Perkin Elmer 100 serial FT-IR spectrophotometer (PerkinElmer, Santa Clara, CA, USA) calibrated with polystyrene film. pH-Titration curves were recorded on a FiveEasy Plus serial pH meter (Mettler Toledo, Switzerland, CH).

Methods

Polymerization setup and polypeptide characterization

DPP-mediated polymerization of NCA was carried out under ambient conditions. For a typical reaction, DPP (0.25 mg, 0.01mmol) was mixed with the $CHCl_3$ solution of BLG-NCA (26.3 mg, 0.1 mmol) into which the $CHCl_3$ solution of C_6-diNH_2 (0.05 mM, 20 μL, 0.01 mmol) ($[M]_0$ = 0.1 M, $[M]_0/[I]_0/[DPP]_0$ = 100/1/1) was added. After complete conversion of NCA as monitored by FT-IR, the resulting polymers were purified by precipitation in hexane/ether (1/1, v/v) and dried under vacuum. The obtained polypeptides were dissolved in DMF containing 0.1 M LiBr, filtered through a 0.45 μm polytetrafluoroethylene (PTFE) membrane (Thermo Fisher Scientific, Waltham, MA, United States), and analyzed by GPC. Polymerization in other solvents, with other monomers, initiators ($[M]_0/[I]_0$ = 40-200) and additives ($[additive]_0/[I]_0$ = 0.01-10) were conducted similarly. To measure the MWs at different monomer conversions, the polymerization was terminated at different time intervals by the addition of trifluoroacetic acid (TFA; 2.5 vol %). The polypeptides were then collected by precipitation, dried, and dissolved in DMF containing LiBr (0.1 M) for GPC analysis.

Synthesis and polymerization of crude BLG-NCA

To a stirred solution of BLG (1.0 g, 4.21 mmol) in THF (15 mL), methyloxirane (1.3 mL, 16.9 mmol) was added sequentially. Triphosgene (0.63 g, 2.11 mmol) was then added in one portion and the vessel was sealed immediately. The solution gradually turned clear in ~30 min with a noticeable heat release and subsequently stirred at room temperature for an additional 1.5 h. The crude BLG-NCA monomers were isolated *via*

precipitation in hexane and dried under vacuum without further purification. This step represents a simplified purification distinct from traditional multi-step recrystallization.

The monomeric chlorine content (reflecting HCl concentration) was determined via SEM-EDS elemental mapping analysis, which provides semi-quantitative evaluation of chlorine (Cl) distribution and concentration at the microscale. This method combines scanning electron microscopy (SEM) for high-resolution imaging and energy-dispersive X-ray spectroscopy (EDS) for elemental composition analysis, enabling simultaneous characterization of surface morphology and Cl distribution. The Cl content was calculated based on characteristic X-ray intensities calibrated against standard references, with mapping performed across representative sample regions to ensure statistical reliability.

Polymerization of crude NCA was carried out under ambient conditions. Typically, DPP (0.25 mg, 0.01 mmol) was mixed with the $CHCl_3$ solution of crude BLG-NCA (26.3 mg, 0.1 mmol) into which the $CHCl_3$ solution of C_6-diNH_2 (0.05 mM, 20 μL, 0.01 mmol) was added. The following procedures of workout was the same as described previously.

Polymerization kinetics

For the polymerization kinetic study, the consumption of NCA was monitored by FT-IR. In a typical FT-IR experiment, the polymerization mixture was transferred into a liquid FT-IR cell after the mixing of the monomer, initiator, and acid. The FT-IR spectra were monitored at different time intervals until the disappearance of anhydride peaks from NCA at 1860 cm^{-1} and 1790 cm^{-1}. The concentration of NCA monomer was then quantified through the standard curve based on the absorbance at 1790 cm^{-1}.

Titration for pH Determination

The pH titration experiments were performed using 1 M NaOH to titrate two phosphate derivatives: diphenyl phosphate (DPP, 0.1 M, 10 mL) and dimethyl phosphate (DMP, 0.01 M, 10 mL). The titration was carried out using a calibrated Class A burette (50 mL for DPP; 10 mL micro burette for DMP to enhance precision), with continuous

magnetic stirring to ensure homogeneity. The titration endpoint was determined by the pH meter reading (>10.0). Each titration was repeated at least twice, and the average volume of NaOH consumed was used to calculate the concentration of DPP and DMP based on stoichiometric ratios. pH meter calibration was performed daily with standard buffers (pH 4.00, 7.00, 10.00).

NOESY studies

NOESY experiments were performed with the "noesygpphpp" pulse sequence, 2D data was collected with four repeated scans and 2048 data points in the direct dimension and 512 increments in the indirect dimension. A relaxation delay of 2 s was used. The mixing time was set to be 0.3 s.

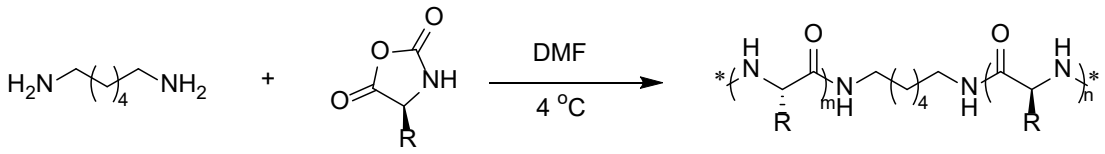

Scheme S1. Synthesis of C_6-di-PBLG$_{30}$ macroinitiators ($[M]_0$ = 0.1 M, $[M]_0/[I]_0$ = 60).

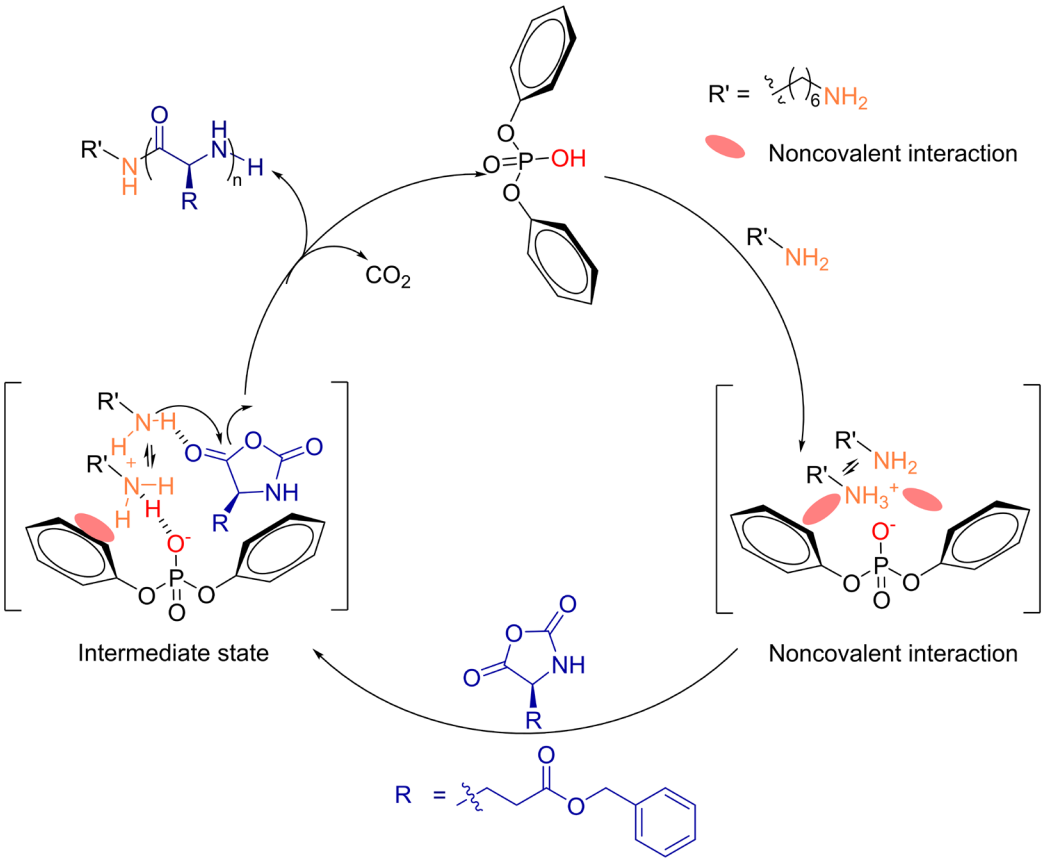

Scheme S2. The proposed mechanism for DPP mediated controlled polymerization.

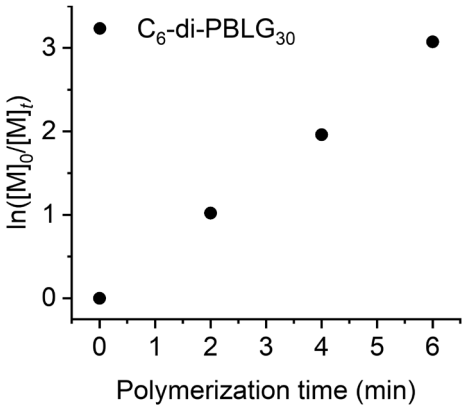

Figure S1. Semilogarithmic kinetic plot illustrating the C_6-di-$PBLG_{30}$-initiated polymerization of BLG-NCA in the absence of DPP in $CHCl_3$ as monitored by FT-IR ($[M]_0$ = 0.1 M, $[M]_0/[I]_0$ = 60).

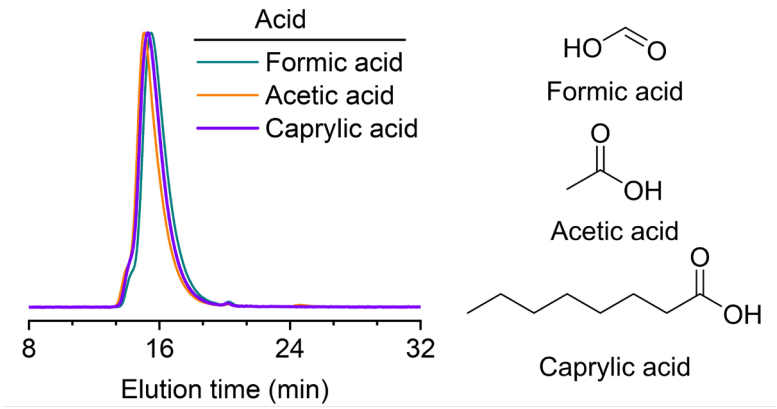

Figure S2. Normalized GPC-LS traces of telechelic PBLG from C_6-diNH_2-initiated polymerization of BLG-NCA in the presence of different acids in $CHCl_3$ ($[M]_0$ = 0.1 M, $[M]_0/[I]_0/[Acid]_0$ = 100/1/1).

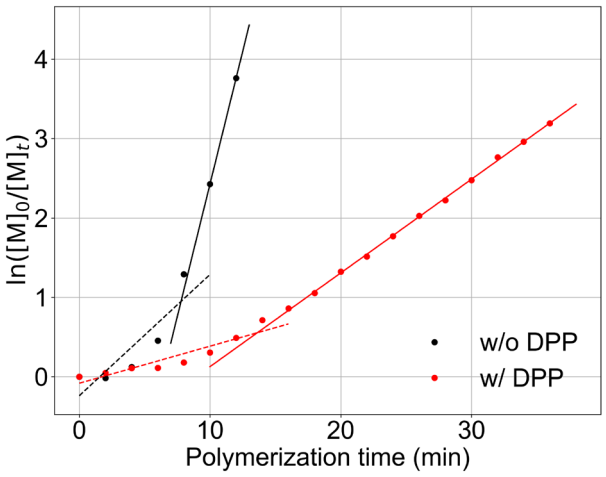

Figure S3. Fitting curves of the semilogarithmic kinetic plot illustrating the C_6-diNH_2-initiated polymerization of BLG-NCA as monitored by FT-IR in the presence and absence of DPP ($[M]_0$ = 0.1 M, $[M]_0/[I]_0/[DPP]_0$ = 100/1/1).

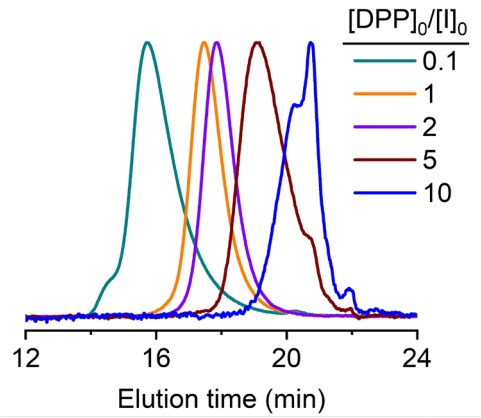

Figure S4. Normalized GPC-LS traces of telechelic PBLG from C_6-diNH_2-initiated polymerization of BLG-NCA in the presence of various equivalents of DPP ($[M]_0$ = 0.1 M, $[M]_0/[I]_0$ = 100).

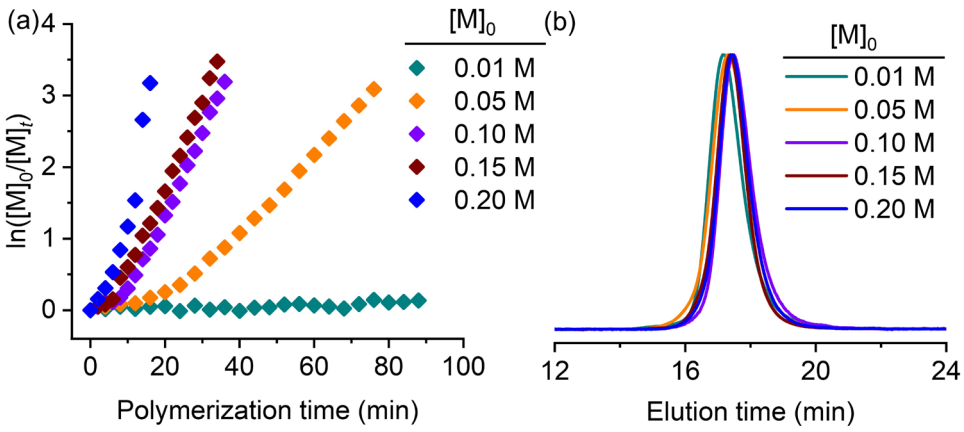

Figure S5. Polymerization of BLG-NCA in $CHCl_3$ with DPP at various monomer concentrations. (a) Semilogarithmic kinetic plot illustrating the C_6-diNH_2-initiated polymerization of BLG-NCA in the presence of DPP at various concentration of monomer in $CHCl_3$ as monitored by FT-IR ($[M]_0/[I]_0/[DPP]_0$ = 100/1/1). (b) Normalized GPC-LS traces of telechelic PBLG from C_6-diNH_2-initiated polymerization of BLG-NCA in the presence of DPP at various concentration of monomer in $CHCl_3$ ($[M]_0/[I]_0/[DPP]_0$ = 100/1/1).

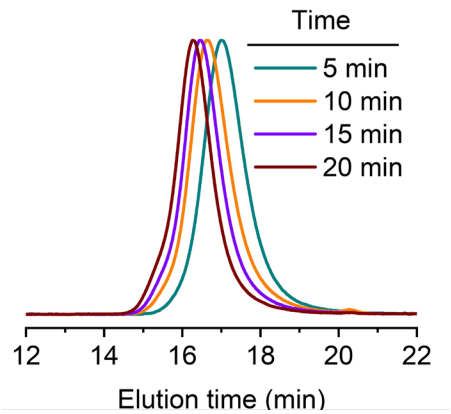

Figure S6. Normalized GPC-LS traces of telechelic PBLG from C_6-di-PBLG$_{50}$-initiated polymerization of BLG-NCA in the presence of DPP in $CHCl_3$ at different time interval ($[M]_0$ = 0.1 M, $[M]_0/[I]_0/[DPP]_0$ = 100/1/1).

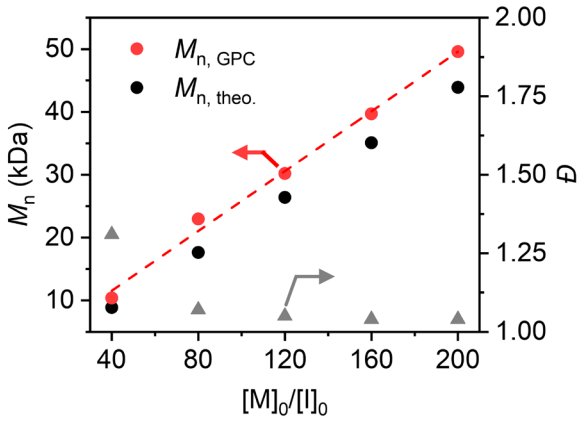

Figure S7. The changes in MWs and dispersity of DPP-mediated ROP of BLG-NCA at various $[M]_0/[I]_0$ in $CHCl_3$ ($[M]_0$ = 0.1 M, $[DPP]_0/[I]_0$ = 1).

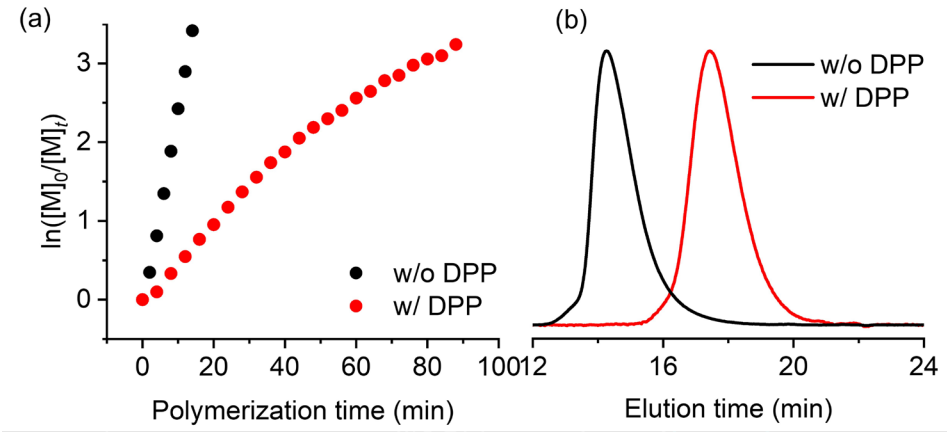

Figure S8. Polymerization of BLG-NCA in the presence and absence of DPP initiated by PEG-diNH_2. (a) Semilogarithmic kinetic plot illustrating the PEG-diNH_2-initiated polymerization of BLG-NCA in the presence and absence of DPP in $CHCl_3$ as monitored by FT-IR ($[M]_0$ = 0.1 M, $[M]_0/[I]_0/[DPP]_0$ = 100/1/2). (b) Normalized GPC-LS traces of telechelic PBLG from PEG-diNH_2-initiated polymerization of BLG-NCA in the presence and absence of DPP in $CHCl_3$ ($[M]_0$ = 0.1 M, $[M]_0/[I]_0/[DPP]_0$ = 100/1/2).

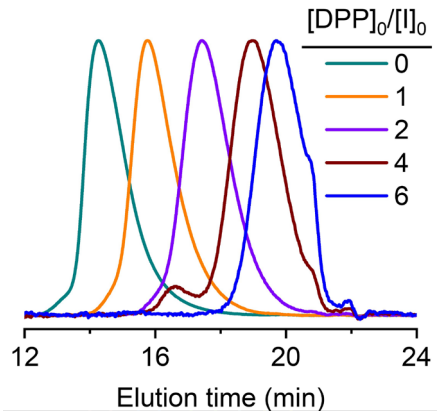

Figure S9. Normalized GPC-LS traces of telechelic PBLG from PEG-diNH_2-initiated polymerization of BLG-NCA in the presence of various equivalents of DPP in $CHCl_3$ ($[M]_0$ = 0.1 M, $[M]_0/[I]_0$ = 100).

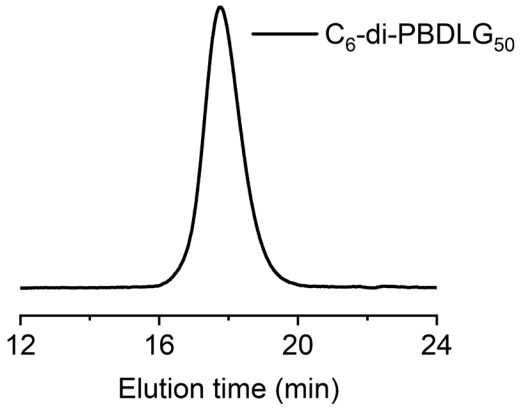

Figure S10. Normalized GPC-LS traces of telechelic PBDLG from C_6-diNH_2-initiated polymerization of BDLG-NCA in the absence of DPP in $CHCl_3$ ($[M]_0$ = 0.1 M, $[M]_0/[I]_0$ = 100).

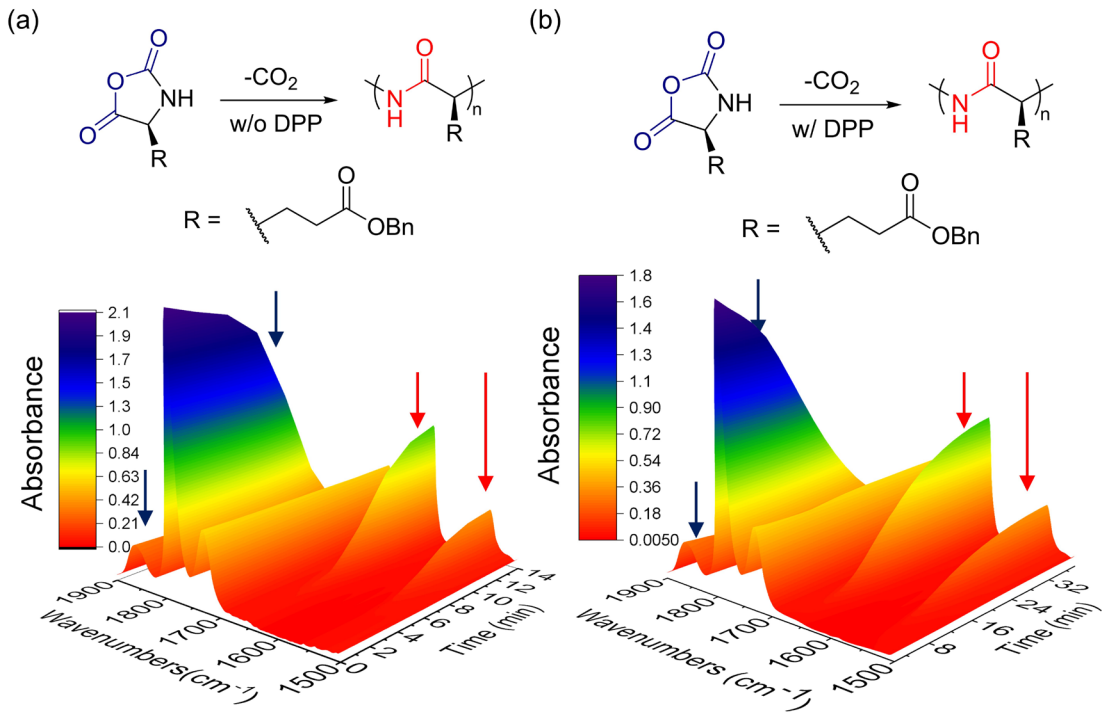

Figure S11. FT-IR-Monitored polymerization kinetics of BLG-NCA in $CHCl_3$ with/without DPP. (a) Changes in the concentration of BLG-NCA and PBLG as monitored by FT-IR over the course of the polymerization of BLG-NCA initiated by C_6-diNH_2 in the absence of DPP in $CHCl_3$ ($[M]_0 = 0.1$ M, $[M]_0/[I]_0 = 100$). (b) Changes in the concentration of BLG-NCA and PBLG as monitored by FT-IR over the course of the polymerization of BLG-NCA initiated by C_6-diNH_2 in the presence of DPP in $CHCl_3$ ($[M]_0 = 0.1$ M, $[M]_0/[I]_0/[DPP]_0 = 100/1/1$).

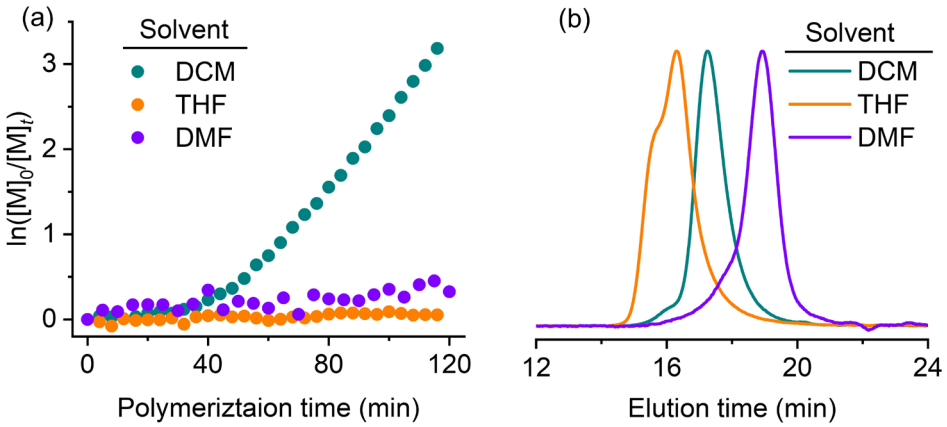

Figure S12. Polymerization of BLG-NCA initiated by C_6-diNH_2 in the presence of DPP in different solvent. (a) Semilogarithmic kinetic plot illustrating the C_6-diNH_2-initiated polymerization of BLG-NCA in the presence of DPP in different solvent as monitored by FT-IR ($[M]_0$ = 0.1 M, $[M]_0/[I]_0/[DPP]_0$ = 100/1/1). (b) Normalized GPC-LS traces of telechelic PBLG from C_6-diNH_2-initiated polymerization of BLG-NCA in the presence of DPP in different solvent ($[M]_0$ = 0.1 M, $[M]_0/[I]_0/[DPP]_0$ = 100/1/1).

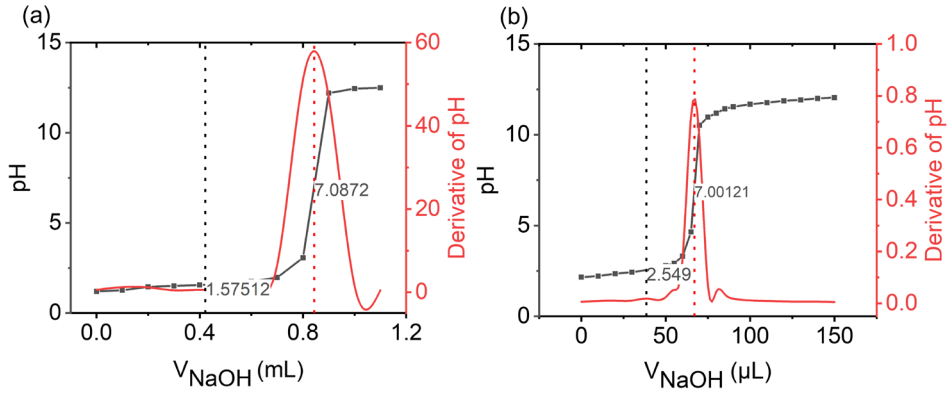

Figure S13. The pH titration curves of (a) DPP and (b) DMP ($[DPP]_0$ = 0.1 M, $[DMP]_0$ = 0.01 M, $[NaOH]_0$ = 0.1 M).

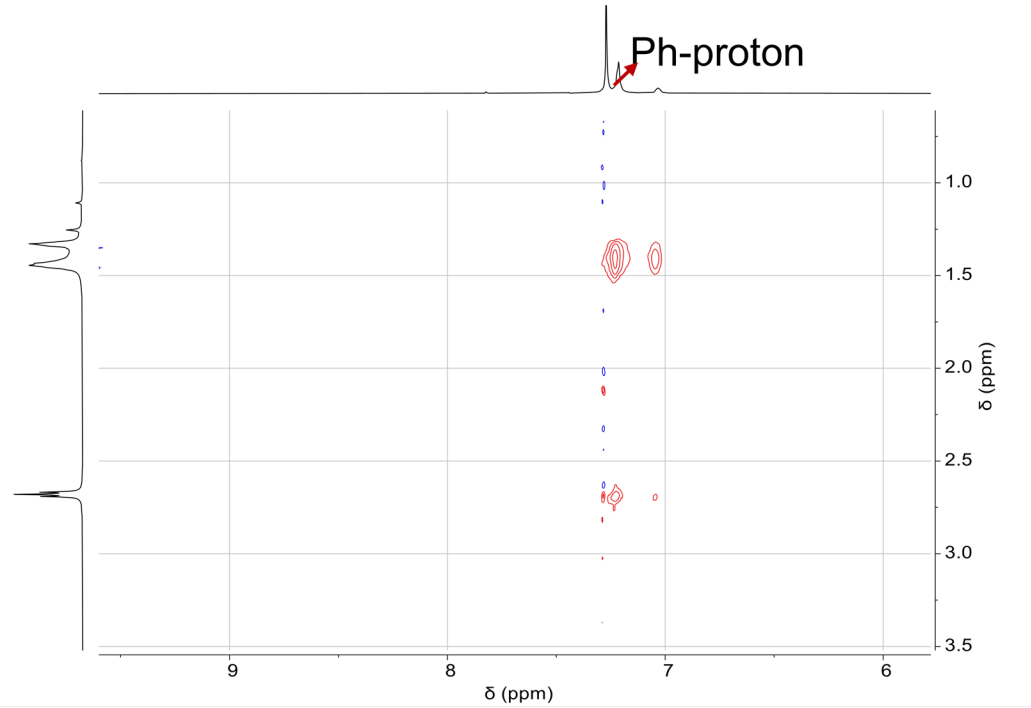

Figure S14. NOESY NMR spectrum of C_6-diNH_2-DPP complexes in $CDCl_3$ ($[DPP]_0/[C_6\text{-di}NH_2]_0 = 1$).

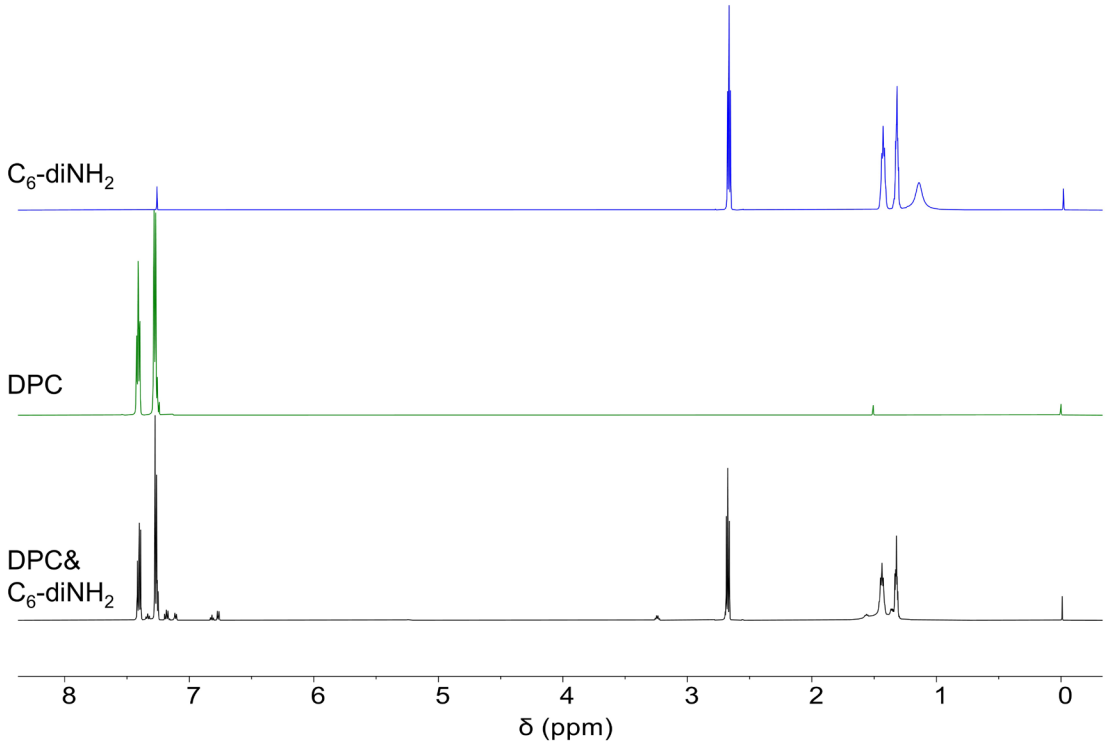

Figure S15. ^{1}H NMR spectra of C_6-diNH_2 (blue curve), DPC (green curve), and C_6-diNH_2 mixed with DPC (black curve, $[DPC]_0/[C_6\text{-di}NH_2]_0 = 1$).

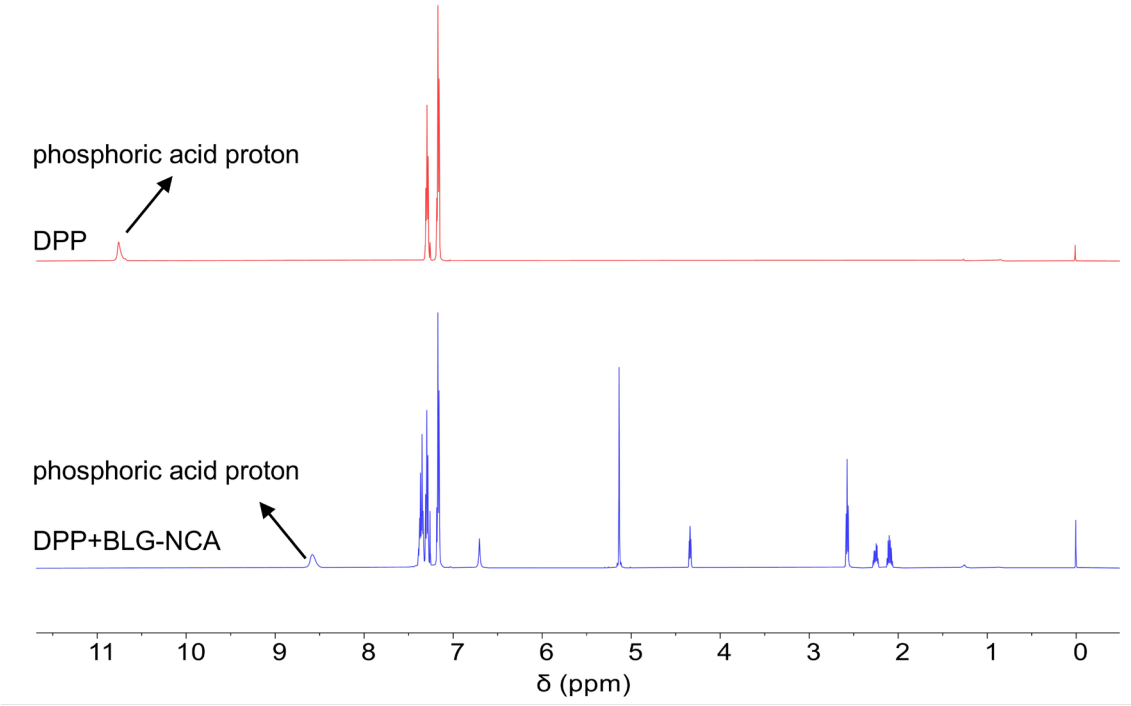

Figure S16. ^{1}H NMR spectra of DPP (red curve) and BLG-NCA mixed with DPP (blue curve, $[DPP]_0/[BLG\text{-}NCA]_0 = 1$).

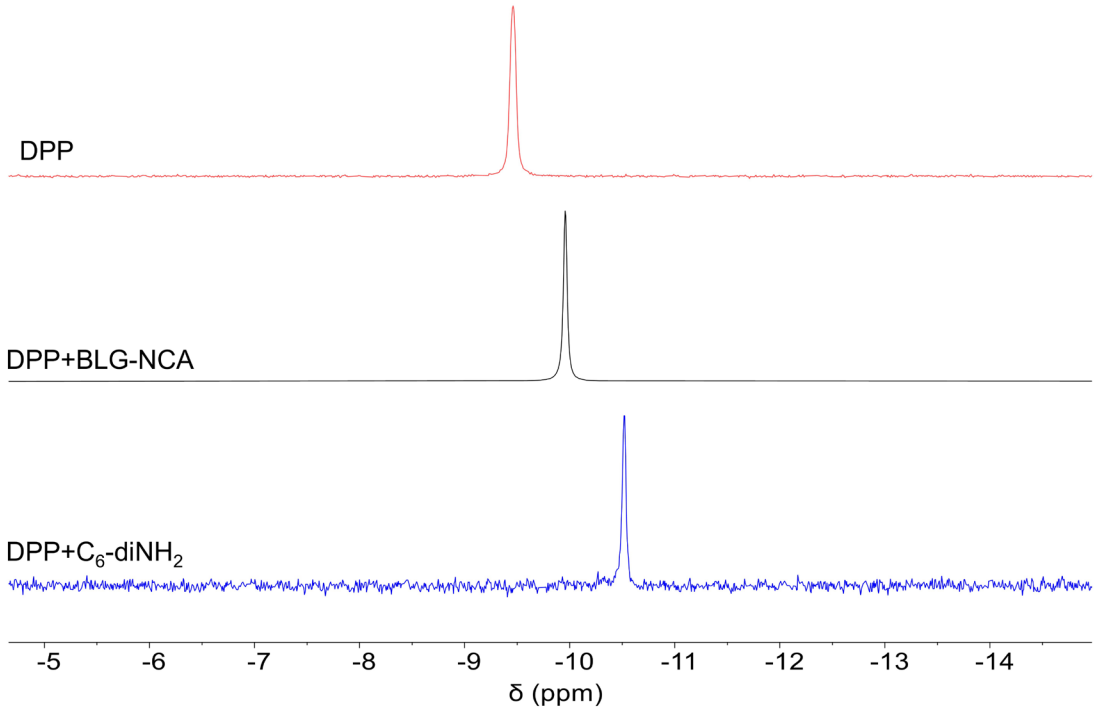

Figure S17. ^{31}P NMR spectra of DPP (red curve), DPP mixed with BLG-NCA (black curve, $[DPP]_0/[BLG\text{-}NCA]_0 = 1$), and DPP mixed with C_6-diNH_2 (blue curve, $[DPP]_0/[C_6\text{-}diNH_2]_0 = 1$).

Table S1 Polymerization of BLG-NCA in the absence of DPP[a]

Entry	$[M]_0/[I]_0$	$M_{n,\,theo.}$ (kDa)	$M_{n,\,GPC}$ (kDa)[b]	$Đ$[b]
1	60	13.3	12.9	1.05
2[c]	60	26.4	27.3	1.06

[a]The monomer conversion was > 95% for both Entry 1 and 2 as determined by FT-IR ($[M]_0$ = 0.1 M).

[b]Determined by GPC; d*n*/d*c* = 0.095

[c]The polymerization was initiated by the macroinitiator obtained from Entry 1 in $CHCl_3$.

Table S2 Polymerization of BLG-NCA in the presence of different acids[a]

Entry	Acid	$M_{n,\ theo.}$ (kDa)	$M_{n,\ GPC}$ (kDa)[b]	$Đ$[b]
1	Formic acid	22.0	48.3	1.22
2	Acetic acid	22.0	59.2	1.22
3	Caprylic acid	22.0	55.2	1.20

[a]All polymerizations were initiated by C_6-diNH_2 ($[M]_0$ = 0.1 M, $[M]_0/[I]_0/[Acid]_0$ = 100/1/1) with monomer conversion > 95% as determined by FT-IR.

[b]Determined by GPC; dn/dc = 0.095.

Table S3 Polymerization of BLG-NCA in the presence of various amounts of DPP[a]

Entry	$[DPP]_0/[I]_0$	t (min)[b]	$M_{n,\,theo.}$ (kDa)	$M_{n,\,GPC}$ (kDa)[c]	$Đ$[c]
1	0.1	35	22.0	46.4	1.17
2	1	35	22.0	25.8	1.07
3	2	180	22.0	22.0	1.06
4	5	1200	22.0	5.34	1.54
5	10	1440	22.0	2.49	1.35

[a]All polymerizations were initiated by C_6-diNH_2 in $CHCl_3$ ($[M]_0$ = 0.1 M, $[M]_0/[I]_0$ = 100).

[b]Polymerization time reaching 95% monomer conversion.

[c]Determined by GPC; dn/dc = 0.095.

Table S4 Polymerization of BLG-NCA in the presence of DPP under various monomer concentrations[a]

Entry	$[M]_0$ (M)	$M_{n,\,theo.}$ (kDa)	$M_{n,\,GPC}$ (kDa)[b]	$Đ^b$
1	0.01	22.0	28.6	1.06
2	0.05	22.0	29.5	1.07
3	0.10	22.0	25.8	1.07
4	0.15	22.0	29.2	1.05
5	0.20	22.0	27.2	1.05

[a]All polymerizations were initiated by C_6-diNH_2 in $CHCl_3$ ($[M]_0/[I]_0/[DPP]_0 = 100/1/1$). The monomer conversion was > 95% for all polymerizations as determined by FT-IR.
[b]Determined by GPC; d*n*/d*c* = 0.095.

Table S5 Polymerization of BLG-NCA in the presence and absence of DPP initiated by different aliphatic diamine[a]

Entry	Initiator	$M_{n,\ theo.}$ (kDa)	$M_{n,\ GPC}$ (kDa)[b]	$Đ$[b]
1[c]	C_3-diNH$_2$	22.0	62.8	1.30
2	C_3-diNH$_2$	22.0	28.7	1.09
3[c]	C_{12}-diNH$_2$	22.0	56.6	1.27
4	C_{12}-diNH$_2$	22.0	27.4	1.05

[a]All polymerizations were initiated in $CHCl_3$ ($[M]_0$ = 0.1 M, $[M]_0/[DPP]_0/[I]_0$ = 100/1/1). The monomer conversion was > 95% for all polymerizations as determined by FT-IR.

[b]Determined by GPC; d*n*/d*c* = 0.095

[c]Polymerization in the absence of DPP.

Table S6 Polymerization of BLG-NCA initiated by PEG-diNH_2 in the presence of various amounts of DPP[a]

Entry	$[DPP]_0/[I]_0$	$M_{n,\,theo.}$ (kDa)	$M_{n,\,GPC}$ (kDa)[b]	$Đ$[b]
1	0	23.0	96.2	1.20
2	1	23.0	44.7	1.19
3	2	23.0	20.3	1.22
4	4	23.0	7.3	1.50
5	6	23.0	2.8	2.15

[a]All polymerizations were initiated in $CHCl_3$ ($[M]_0$ = 0.1 M, $[M]_0/[I]_0$ = 100). The monomer conversion was > 95% for all polymerizations as determined by FT-IR.
[b]Determined by GPC; dn/dc = 0.095.

Table S7 Polymerization of BLG-NCA initiated by PEG-diNH_2 at various $[M]_0/[I]_0$[a]

Entry	$[M]_0/[I]_0$	$M_{n,\,theo.}$ (kDa)	$M_{n,\,GPC}$ (kDa)[b]	$Đ$[b]
1	40	8.7	8.9	1.40
2	80	17.5	16.7	1.26
3	120	27.2	22.6	1.21
4	160	36.0	28.8	1.16
5	200	44.8	34.5	1.15

[a]All polymerizations were initiated in $CHCl_3$ ($[M]_0$ = 0.1 M, $[DPP]_0/[I]_0$ = 2). The monomer conversion was > 95% for all polymerizations as determined by FT-IR.
[b]Determined by GPC; dn/dc = 0.095.

Table S8 Block Polymerization of BLG-NCA (monomer of Block A), ELG-NCA (monomer of Block B), and ZLL-NCA (monomer of Block C) in the presence of DPP[a]

Entry	Block	$M_{n,\,theo.}$ (kDa)	$M_{n,\,GPC}$ (kDa)[b]	$Đ^b$
1	ABC	38.2	38.7	1.06
2	ABCA	51.3	53.1	1.08
3	ABCAB	60.5	62.3	1.05

[a]All polymerizations were initiated by C_6-diNH_2 in $CHCl_3$ ($[M]_0$ = 0.1 M, $[M]_0/[I]_0/[DPP]_0$ = 60/1/1). The monomer conversion was > 95% for all polymerizations as determined by FT-IR.

[b]Determined by GPC; d*n*/d*c* = 0.095.

Table S9 Polymerization of BLG-NCA initiated in the presence of DPP in different solvent[a]

Entry	Solvent	$M_{n,\ theo.}$ (kDa)	$M_{n,\ GPC}$ (kDa)[b]	$Đ$[b]
1	DCM	22.0	28.2	1.09
2	THF	22.0	51.6	1.07
3	DMF	22.0	14.4	1.09

[a]All polymerizations were initiated by C_6-diNH_2 ($[M]_0$ = 0.1 M, $[M]_0/[I]_0/[DPP]_0$ = 100/1/1). The monomer conversion was > 95% for all polymerizations as determined by FT-IR.

[b]Determined by GPC; dn/dc = 0.095.

Table S10 Polymerization of BLG-NCA in the presence of DPC and DMP[a]

Entry	Additive	$M_{n,\,theo.}$ (kDa)	$M_{n,\,GPC}$ (kDa)[b]	$Đ$[b]
1	DPC	22.0	83.6	1.14
2	DMP	22.0	63.8	1.05

[a]All polymerizations were initiated by C_6-diNH_2 in $CHCl_3$ ($[M]_0$ = 0.1 M, $[M]_0/[I]_0/[Additive]_0$ = 100/1/1). The monomer conversion was > 95% for all polymerizations as determined by FT-IR.

[b]Determined by GPC; d*n*/d*c* = 0.095.

Table S11 EDS element analysis of (a) crude NCA, and (b) purified NCA

(a)

Element Signal	Atomic %	σ
C	75.72	
O	18.26	
N	5.78	
Cl	0.24	

(b)

Element Signal	Atomic %	σ
C	75.27	
O	19.38	
N	5.33	
Cl	0.02	

Table S12 Polymerization of crude BLG-NCA in the presence of DPP[a]

Entry	$[M]_0/[I]_0$	$M_{n,\ theo.}$ (kDa)	$M_{n,\ GPC}$ (kDa)[b]	$Đ$[b]
1[c]	100	22.0	36.7	1.13
2	100	22.0	24.2	1.09
3	40	8.9	11.2	1.31
4	80	17.6	23.6	1.12
5	120	26.4	30.6	1.08
6	160	35.2	36.6	1.07
7	200	43.9	42.0	1.05

[a]All polymerizations were initiated by C_6-diNH_2 in $CHCl_3$ ($[M]_0$ = 0.1 M, $[DPP]_0/[I]_0$ =1). The monomer conversion was > 95% for all polymerizations as determined by FT-IR.

[b]Determined by GPC; d*n*/d*c* = 0.095

[c]Polymerization in the absence of DPP.

References

(1) Tian, Z. Y.; Zhang, Z.; Wang, S.; Lu, H. A Moisture-Tolerant Route to Unprotected α/β -Amino Acid *N*-Carboxyanhydrides and Facile Synthesis of Hyperbranched Polypeptides. *Nat. Commun.* **2021**, *12*, 5810.

(2) Sun, X.; Li, A.; Li, N.; Ji, G.; Song, Z. Facile Preparation of Heteropolypeptides from Crude Mixtures of α-Amino Acid *N*-Carboxyanhydrides. *Biomacromolecules* **2024**, *25*, 6093-6102.